Study on improvements of the five-point double-toggle mould clamping mechanism

W Y Lin and K M Hsiao

Proceedings of the Institution of Mechanical Engineers, Part C: Journal of Mechanical Engineering Science 2004 218: 761
DOI: 10.1243/0954406041319482

Study on improvements of the five-point double-toggle mould clamping mechanism

W Y Lin[1]* and **K M Hsiao**[2]
[1]Department of Mechanical Engineering, De Lin Institute of Technology, Tucheng, Taiwan
[2]Department of Mechanical Engineering, National Chiao Tung University, Hsinchu, Taiwan

Abstract: In current designs of the conventional and Fanuc five-point double-toggle mechanisms, the lengths of moving-platen side links are greater than the lengths of tailstock-platen side links in order to provide enough horizontal space for the ejector unit and to avoid the unsound transmission characteristic. In this study, another method to provide such a space is adopted. From a parametric study, the method can be proved practicable and the individual profiles of toggle linkages for the two types of mechanism with the characteristics of time saving or a larger opening stroke and/or thrust saving can be found. Moreover, objective comparisons of the performances between the two types of mechanism are also given.

Keywords: five-point double-toggle mould clamping mechanism, injection-moulding machines

NOTATION

a, b, c, k_i $(i = 1–4)$	parameters defined in equation (36)
a_A, a_E	accelerations of the moving platen and the crosshead
A_1, A_2, A_c	cross-sectional areas of link 1, link 2 and the tie bar
d_A	vertical distance between point C and point A
d_E	vertical distance between point C and point E
d_f	vertical distance between the centre-line of the machine and the upper surface of the frame
d_0	vertical distance between the centre-line of the machine and point C
e_1, e_2	distances defined in Fig. 8
E_1, E_2, E_c	Young's modulus of link 1, link 2 and the tie bar
F_{AB}, F_{BF}, F_{CF}	axial forces in a single link 1, the segments BF and CF of a single link 2
F_{cl}	clamping force
F_{ij}, M_{ij} $(i, j = 1–6)$	forces and moments exerted by all members i on a single member j
F_o	thrust applied to the crosshead
F_o^0	thrust applied to the crosshead at the beginning of the mould clamping operation
$F_{o,\,max}$	maximum value of the thrust F_o during the real mould clamping process
$F_{o,\,max}^p$	minimum value of $F_{o,\,max}$ in each case of L_1/L_2
g	acceleration of gravity
h, h_{ej}	horizontal nearest distances between point B and the left end of the ejector unit defined in Fig. 8
h_{CE}^0	horizontal distance between point E and point C in the initial position
L_c	length of the tie bar
L_{CF}	distance between points C and F
L_i $(i = 1–4)$	distances between points A and B, B and C, D and E and C and D
m_6	mass of the moving platen with the ejector unit and the moving mould
M_a	mechanical advantage
n_c	number of the tie bar
n_i $(i = 1–4)$	number of member i
r_B, r_C, r_D	radii of pin joints B, C and D
R_B, R_D	semi-widths of links 1 and the crosshead links

The MS was received on 26 August 2003 and was accepted after revision for publication on 19 March 2004.
* *Corresponding author: Department of Mechanical Engineering, De Lin Institute of Technology, 1 Alley 380, Ching Yun Road, Tucheng, Taiwan.*

S_E, S_A	displacements of the crosshead and the moving platen
T_h, T_m, T_s	dimensions defined in Figs 1 and 2
T_v	overall height (vertical length) of the machine
U_c	elongation of the tie bars
$\overline{U}_c$	parameter defined in equation (17)
v_A, v_E	velocities of the moving platen and the crosshead
$\alpha, \beta, \gamma, \gamma_C, \phi$	angles defined in Figs 4 and 5
$\dot{\alpha}, \ddot{\alpha}$	angular velocity and angular acceleration of link 2
$\alpha_c, \beta_c, \phi_c$	angles α, β and ϕ in the position when the moving mould is just in contact with the stationary mould
$\alpha_0, \beta_0, \phi_0$	angles α, β and ϕ in the initial position
$\overline{\beta}$	angle defined in equation (48)
β_μ, ϕ_μ	angles defined in Fig. 6
$\delta_{AB}, \delta_{BC}, \delta_{DE}$	axial shortened lengths of link 1, link 2 and the crosshead link
δ_{BF}, δ_{CF}	shortened lengths of axial segments BF and CF of links 2
$\Delta h, \Delta h^0_{CE}$	parameters defined in equations (50) and (51)
$\Delta T_h, \Delta T_v$	increments of the overall horizontal length and height of the machine
μ, μ_s	kinetic and static friction coefficients
ρ_B, ρ_C, ρ_D	friction radii of pin joints B, C and D
$(\ )^0$	quantity in the state of the initial position of the mould clamping process
$(\ )^c$	quantity at the time of the contact position
$(\tilde{\ })$	quantity in the state of the final position of the mould clamping process
$(\ )^*$	quantity only for the original mechanism

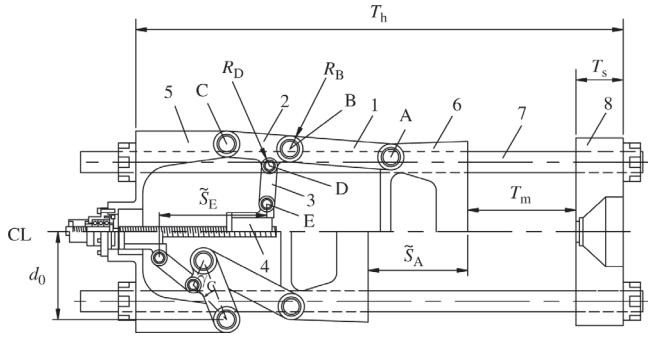

Fig. 1 Conventional five-point double-toggle mould clamping mechanism

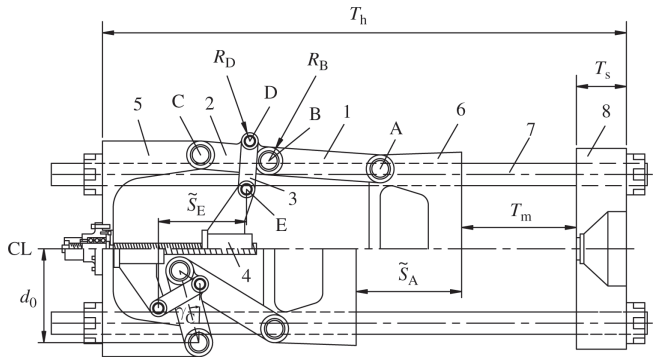

Fig. 2 Fanuc five-point double-toggle mould clamping mechanism

1 INTRODUCTION

The conventional five-point double-toggle mould clamping mechanism as shown in Fig. 1 is extensively used for injection-moulding machines with a clamping force of between about 490 kN (50 metric tons) and 4900 kN (500 metric tons) [**1**, **2**]. Fanuc Japan Company Limited developed a new five-point double-toggle mould clamping mechanism shown in Fig. 2 and took out a US Patent in 1998 [**3**]. Note that no quantitative results were reported in reference [**3**]. The extent of the superiority of Fanuc's five-point double-toggle mould clamping has not been shown in the literature. In Figs 1 and 2, the upper portion above the centre-line (CL) of each mould clamping mechanism illustrates a mould closing state with the toggle fully extended in a straight line but no real mould clamping, while the lower portion below the centre-line (CL) illustrates the maximum stroke of mould opening of each mould clamping mechanism.

Constructions common to the conventional and Fanuc five-point mould clamping mechanisms will be described in brief [**3**]. Let numerals 1 to 8 shown in Figs 1 and 2 denote moving-platen side links (links 1), tailstock-platen side links (links 2), crosshead links (links 3), crosshead (4), tailstock platen (5), moving platen (6), tie bars (7), stationary platen (8) and ejector unit (9, not shown in Figs 1 and 2) respectively in this study. A stationary platen (8) is fixed to the injection-moulding machine body (frame) and four tie bars (7) are immovably fixed individually to the four corners of the stationary platen. A tailstock platen (5), mounted on the (precision ground) steel band fixed on the frame, is attached to the respective end portions of the tie bars. A moving platen (6), mounted by the support blocks (or rollers) on the (precision ground) steel band fixed on the frame, is fitted on the tie bars and is able to slide. As two

sets of toggle links, which are formed of links 1 and links 2, are bent or stretched synchronously, the moving platen moves towards or away from the tailstock platen, causing the mould opening or closing operation to be performed. A crosshead (4), which is movable straight in the mould opening or closing direction by means of a drive mechanism composed of a ball nut-screw (or hydraulic ram, etc.), is on the centre-line (CL) intermediate between the two sets of toggle links that are vertically juxtaposed. The respective distal ends of two sets of crosshead links (3) that are pivotally mounted on the upper and lower sides of the crosshead, pull in or push out joint portions of the toggle links, depending on the moving direction of the crosshead. In the last stage of the mould closing operation, the tailstock platen will move away from the moving platen and the tie bars will be stretched after contact between the moving mould attached to the moving platen and the stationary mould attached to the stationary platen. This part of the mould closing operation is called real mould clamping in this paper. Points A to E denote centres of pin joints. The difference between the conventional and Fanuc five-point clamping mechanisms is described in the following. On link 2 of the conventional five-point type shown in Fig. 1, the projection is formed at an inside position (towards the crosshead) on the portion of link 2 that is near joint B. On the other hand, for link 2 of the Fanuc five-point type shown in Fig. 2, the projection is formed at an outside position (outward from the crosshead) on the portion of link 2 that is near joint B. The angles between the vector ***CD*** and the vector ***CB*** in the conventional and Fanuc five-point types are both denoted γ_C, measured positive as shown in Figs 1 and 2 for the former and the latter respectively.

The design of a toggle mould clamping mechanism demands: (a) a large opening stroke (output stroke), (b) a short time for mould opening and (c) a large mechanical advantage. The time for mould opening (or closing) operation is related to the stroke of the crosshead (input stroke) and the velocity of the moving platen. Note that the input and output strokes, in practice, are defined in the mould closing operation without real mould clamping. The demand for an increase in mechanical advantage is equivalent to the demand for a decrease in the necessary maximum thrust applied to the crosshead during the real mould clamping operation. In the current designs of the conventional and Fanuc five-point double-toggle mechanisms, the lengths of moving-platen side links are greater than the lengths of tailstock-platen side links in order to provide enough horizontal space for the ejector unit and to avoid the unsound transmission characteristic. Another feature of profiles of the toggle linkages in the current design is the projection joint D at an inside or outside position on the portion of link 2 near joint B, so that the length of the flange of the tailstock platen is fairly wide (see Figs 1 and 2) and the initial position of point E is as near the tailstock platen as possible to satisfy the desired opening stroke.

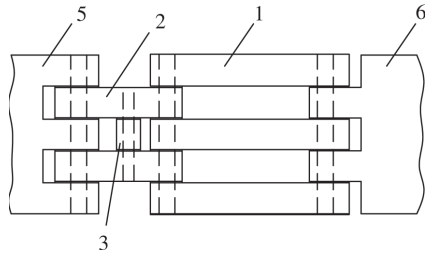

Fig. 3 Method for connections of links 1, links 2 and crosshead links 3

The aims of this study are to adopt another method to provide enough horizontal space for the ejector unit and to use a parametric study to prove the method practicable and to find the individual profiles of the toggle linkages of the two types of mechanism with the characteristics of time saving or larger opening stroke and/or thrust saving as improvements on them. Moreover, an objective comparison of the performances between the two types of mechanism is also given. Note that the analytical model of the conventional five-point type is common to that of the Fanuc five-point type. If the formulation for the conventional five-point type is established, the formulation for the Fanuc five-point type can be obtained by replacing the angle γ_C of the formulation of the conventional five-point type with the angle $-\gamma_C$. Unless otherwise stated, only the model for the conventional five-point type is presented in this paper. For comparison, the method for connecting links 1 and links 2 shown in Fig. 3, which is a schematic plan view, is used in the conventional and Fanuc five-point clamping mechanisms.

2 INPUT STROKE AND OUTPUT STROKE

The degree of freedom for the five-point double-toggle mechanism is one that can be obtained from Grueblertype formulae [**4**, **5**]. Figure 4 depicts a skeleton drawing for the lower half of the conventional five-point double-toggle mould clamping mechanism. The solid lines denote the position during the mould closing operation without real mould clamping and the dashed lines denote the maximum mould opening state, i.e. the initial position. The final position for the mould closing operation is achieved when the toggle is fully extended in a straight line. In this study, the symbol $(\tilde{})$ denotes that the quantity in parentheses is in the state of the final position of the mould closing operation.

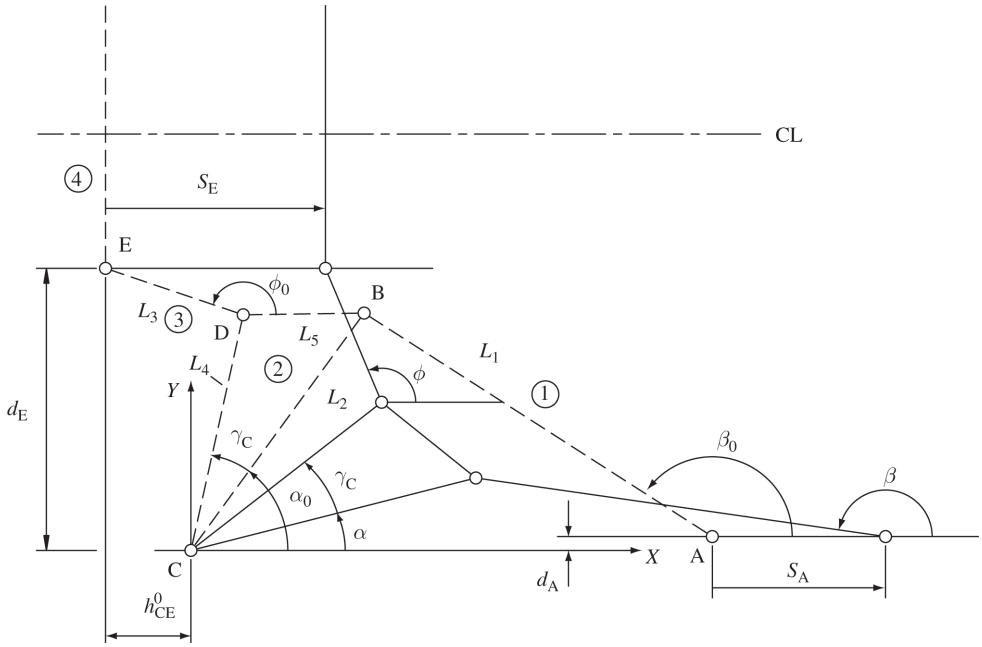

Fig. 4 Geometry of the conventional toggle linkage during mould closing

From Fig. 4 and the geometry of the final position of the mould closing operation,

$$L_2 \sin\alpha_0 - L_1 \sin(\pi - \beta_0) = L_2 \sin\alpha - L_1 \sin(\pi - \beta) = d_A \quad (1)$$

$$L_4 \sin(\alpha_0 + \gamma_C) + L_3 \sin(\pi - \phi_0) = L_4 \sin(\alpha + \gamma_C) + L_3 \sin(\pi - \phi) = d_E \quad (2)$$

$$\tilde{\beta} = \tilde{\alpha} + \pi \quad (3)$$

$$S_E = L_4[\cos(\alpha + \gamma_C) - \cos(\alpha_0 + \gamma_C)] + L_3[\cos(\pi - \phi_0) - \cos(\pi - \phi)] \quad (4)$$

$$S_A = L_1[\cos(\pi - \beta) - \cos(\pi - \beta_0)] + L_2(\cos\alpha - \cos\alpha_0) \quad (5)$$

$$v_E = -L_4[\sin(\alpha + \gamma_C) + \cos(\alpha + \gamma_C)\tan(\pi - \phi)]\dot{\alpha} \quad (6)$$

$$v_A = -L_2[\sin\alpha + \cos\alpha \tan(\pi - \beta)]\dot{\alpha} \quad (7)$$

$$a_E = -L_4[\sin(\alpha + \gamma_C) + \cos(\alpha + \gamma_C)\tan(\pi - \phi)]\ddot{\alpha} - L_4\left[\cos(\alpha + \gamma_C) - \sin(\alpha + \gamma_C)\tan(\pi - \phi) - \frac{L_4 \cos^2(\alpha + \gamma_C)}{L_3 \cos^3(\pi - \phi)}\right]\dot{\alpha}^2 \quad (8)$$

$$a_A = -L_2[\sin\alpha + \cos\alpha \tan(\pi - \beta)]\ddot{\alpha} - L_2\left[\cos\alpha - \sin\alpha \tan(\pi - \beta) + \frac{L_2 \cos^2\alpha}{L_1 \cos^3(\pi - \beta)}\right]\dot{\alpha}^2 \quad (9)$$

$$h^0_{CE} = L_3 \cos(\pi - \phi_0) - L_4 \cos(\alpha_0 + \gamma_C) \quad (10)$$

where L_i ($i = 1$–4) are the distances between points A and B, B and C, D and E and C and D respectively at the undeformed state of the mechanism; S_E and S_A are the displacements of the crosshead and the moving platen respectively; $\dot{\alpha}$ and $\ddot{\alpha}$ are the angular velocity and angular acceleration of links 2 respectively; v_A and v_E are the velocities of the moving platen and the crosshead respectively; a_A and a_E are the accelerations of the moving platen and the crosshead respectively; h^0_{CE} is the horizontal distance between point E and point C in the initial position, measured positive if the former is to the left of the latter.

The expressions for the input stroke $\widetilde{S}_E$ and the output stroke, or the so-called opening stroke $\widetilde{S}_A$, can be obtained using equations (1) to (5). In this study, the values of $d_A, d_E, L_1, L_2, L_4, \widetilde{S}_A, \widetilde{S}_E$ and $\tilde{\phi}$ are prescribed. The values of $\tilde{\alpha}$ and $\tilde{\beta}$ can be obtained from equations (1) and (3). The values of α_0, β_0 and ϕ_0 can be obtained from the expression for $\widetilde{S}_A$ and equations (1) and (2). The values of γ_C and L_3 can be obtained from the expression for $\widetilde{S}_E$ and equation (2).

3 ELASTOSTATIC MODEL

The necessary maximum thrust applied to the crosshead, which reflects the performance of mechanical advantage of a toggle mould clamping mechanism, should occur in the course of the real mould clamping operation. Thus, only the real mould clamping operation is considered in this section. In the course of the real mould clamping, in order to develop the clamping force, the toggle clamping mechanism must overcome the friction forces in pin joints (hinge friction) and slider connections, and the total deformation force of the tie bars. Here, the slider

connections comprise the crosshead and the guide rods, and the tailstock platen and the (precision ground) steel bands. In practice, the design of the toggle mould clamping mechanism tends towards rugged. However, the effect of the toggle linkage deformation should be considered unless the stiffness of the toggle linkage is very much greater than that of the tie bars. Moreover, the effect of hinge friction should not be negligible for the mould clamping operation [**5**]. Hydrodynamic lubrication between toggle pins and bushings cannot be achieved due to the reciprocating motion of the toggle mechanism and heavy contact forces. The lubrication between the two members may be considered as boundary or thin-film lubrication. A partial breakdown of a thin oil or grease film between the two members usually occurs during real mould clamping, because of heavy forces. Such a situation may cause direct physical contact and rubbing between two metal members. This type of friction may be considered as Coulomb friction [**6**]. Conservatively, it may be reasonable to assume that Coulomb friction in the pin joints is valid for the mould clamping operation [**5**]. To achieve the desired clamping force, the velocity is always reduced to a very low value in the course of real mould clamping. The following assumptions are made:

1. The axial deformation displacements of links and tie bars are small, and the flexural deformations of links and tie bars are negligible.
2. The inertia forces, the weights and the friction forces in the slider connections can be neglected when compared to the total deformation force of the tie bars and the thrust of the crosshead.
3. The deformation effects of the mould and the mould platens are negligible.
4. Coulomb friction is valid for the friction in pin joints.
5. The friction coefficients are the same for all pin joints.

Due to assumption 1, the equilibrium equations of the toggle clamping system are constructed at the undeformed configuration of the toggle clamping system during the real mould clamping operation in this study.

Figure 5 depicts a skeleton drawing for the lower half of the conventional five-point double-toggle mould clamping mechanism during the real mould clamping operation. The dashed lines denote the position when the moving mould is just in contact with the stationary mould. It is assumed that the toggle mechanism and the tie bars are not yet deformed in this state. After contact, the toggle linkage is subjected to compressive force. Thus, besides the rigid-body motion, compressive deformation arises for the toggle linkage. As can be seen from the solid line shown in Fig. 5, the moving platen is at rest and the tailstock platen moves backwards after contact. The final position for the real mould clamping operation is achieved when the toggle is fully extended in a straight line.

From Fig. 5, the geometry of the final position of the real mould clamping operation and the assumption of small deformation give

$$\begin{aligned} & L_2 \sin \alpha_c - L_1 \sin(\pi - \beta_c) \\ & \quad = (L_2 - \delta_{BC}) \sin \alpha - (L_1 - \delta_{AB}) \sin(\pi - \beta) \\ & \quad = d_A \end{aligned} \tag{11}$$

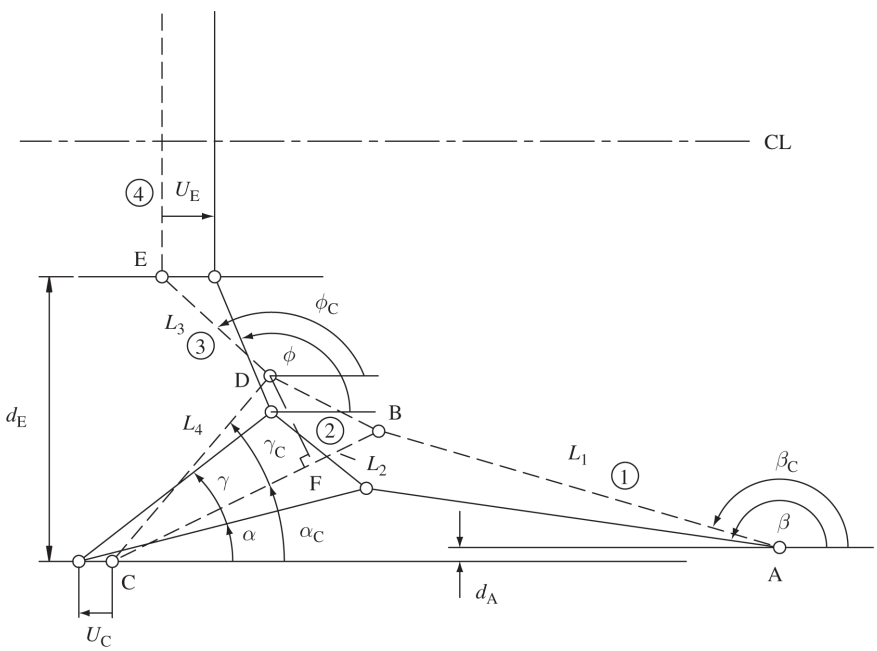

Fig. 5 Geometry of the conventional toggle linkage during real mould clamping

$$L_4\sin(\alpha_c+\gamma_C)+L_3\sin(\pi-\phi_c)=(L_{CF}-\delta_{CF})\sin\alpha+L_4\sin\gamma_C\cos\alpha+(L_3-\delta_{DE})\sin(\pi-\phi)=d_E \quad (12)$$

$$\widetilde{\beta}=\widetilde{\alpha}+\pi \quad (13)$$

$$L_{CF}=L_4\cos\gamma_C \quad (14)$$

$$\tan\gamma=\frac{L_4\sin\gamma_C}{L_{CF}-\delta_{CF}} \quad (15)$$

$$U_c=(L_1-\delta_{AB})\cos(\pi-\beta)-L_1\cos(\pi-\beta_c)+(L_2-\delta_{BC})\cos\alpha-L_2\cos\alpha_c=\overline{U}_c-\delta_{AB}\cos(\pi-\beta)-\delta_{BC}\cos\alpha \quad (16)$$

$$\overline{U}_c=L_1[\cos(\pi-\beta)-\cos(\pi-\beta_c)]+L_2(\cos\alpha-\cos\alpha_c) \quad (17)$$

where L_{CF} is the distance between point C and point F at the undeformed state of the mechanism, U_c is the elongation of the tie bars, δ_{AB}, δ_{BC} and δ_{DE} are the axial shortened lengths of links 1, 2 and 3 respectively and δ_{BF} and δ_{CF} are the shortened lengths of axial segments BF and CF of links 2 respectively. Due to the assumption of small deformation, $\delta_{AB}, \delta_{BC}, \delta_{DE}$ and δ_{CF} in equations (11), (12) and (15) are dropped in this study. Thus, the values of $\widetilde{\alpha}, \widetilde{\beta}$ and $\widetilde{\phi}$ and $\gamma=\gamma_C$ can be obtained using equations (11) to (15).

Let F_{ij} shown in Fig. 6 represent the force exerted by all members i on a single member j. The circles shown in Fig. 6 are called friction circles [**5**, **6**]. For the sake of clarity, the friction circles in Fig. 6 have been greatly exaggerated in magnitude. From Figs 1 and 6, the free-body diagrams for each member and joint can be easily drawn (not shown) and the equations of equilibrium required for the real mould clamping operation are given as follows:

$$n_2F_{12}=n_1F_{21}=n_1F_{61}=F_{16} \quad (18)$$

$$F_{cl}=F_{16}\cos(\pi-\beta+\beta_\mu) \quad (19)$$

$$n_4F_{34}=n_3F_{43}=n_3F_{23}=n_2F_{32} \quad (20)$$

$$F_o=n_4F_{34}\cos(\pi-\phi-\phi_\mu) \quad (21)$$

$$F_{52x}=F_{12}\cos(\pi-\beta+\beta_\mu)-F_{32}\cos(\pi-\phi-\phi_\mu) \quad (22)$$

$$F_{52y}=F_{32}\sin(\pi-\phi-\phi_\mu)-F_{12}\sin(\pi-\beta+\beta_\mu) \quad (23)$$

$$M_{52}=F_{32}[L_4\sin(\pi+\alpha+\gamma-\phi-\phi_\mu)+\rho_D]-F_{12}[L_2\sin(\pi+\alpha-\beta+\beta_\mu)+\rho_B]=\rho_C\sqrt{F_{52x}^2+F_{52y}^2}\geqslant 0 \quad (24)$$

$$F_c=n_2F_{52x} \quad (25)$$

$$\beta_\mu=\sin^{-1}\left(\frac{2\rho_B}{L_1}\right),\qquad \phi_\mu=\sin^{-1}\left(\frac{2\rho_D}{L_3}\right) \quad (26)$$

$$\rho_B=\frac{\mu}{\sqrt{1+\mu^2}}r_B,\qquad \rho_C=\frac{\mu}{\sqrt{1+\mu^2}}r_C,\qquad \rho_D=\frac{\mu}{\sqrt{1+\mu^2}}r_D \quad (27)$$

where n_i $(i=1\text{–}4)$ is the number of members i. In equation (19), F_{cl} is the clamping force shown in Fig. 1. In equation (21), F_o is the thrust transmitted to the crosshead. In equation (25), F_c is the total tension force

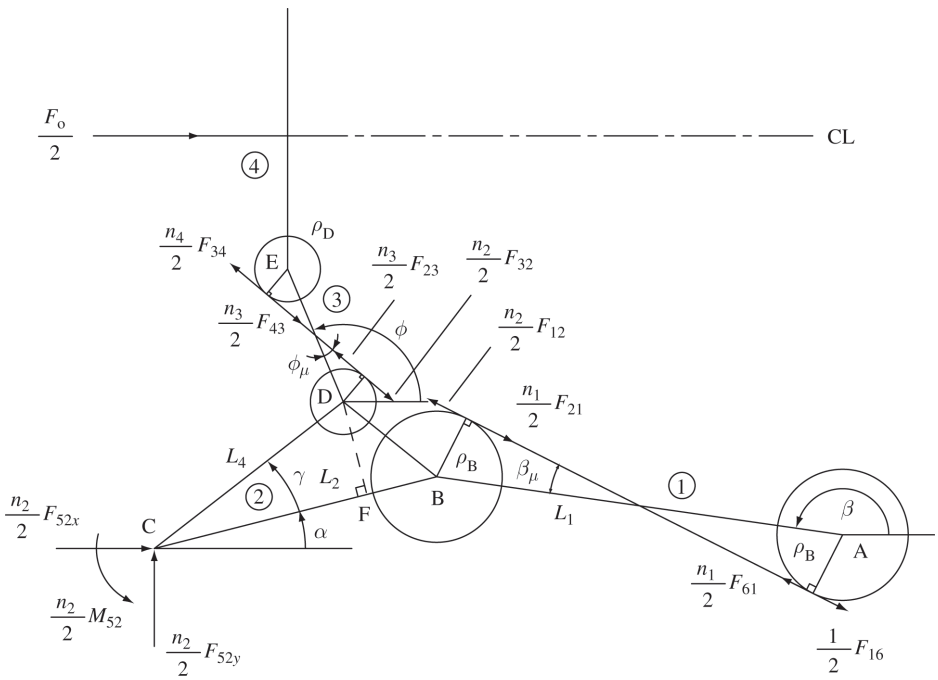

Fig. 6 Conventional toggle linkage subjected to loading during real mould clamping

of the tie bars. In equation (27), μ is the friction coefficient in all pin joints, r_B, r_C and r_D are the radii of pin joints B, C and D respectively and ρ_B, ρ_C and ρ_D are the corresponding friction radii [**5**, **6**] respectively. Note that the radius of joint A is equal to that of joint B and the radius of joint E is equal to that of joint D. M_{52} in equation (24) must be non-negative, because the rotation of links 2 is clockwise during the mould clamping operation.

From equations (18) and (19) and Fig. 6, the compressive axial force in a single link 1 may be expressed as

$$F_{AB} = \frac{F_{cl}\cos\beta_\mu}{n_1\cos(\pi-\beta+\beta_\mu)} \tag{28}$$

From equations (18) to (21) and Fig. 6, the compressive axial force in the segments BF and CF of a single link 2 may be expressed as

$$F_{BF} = \frac{F_{cl}\cos(\pi+\alpha-\beta+\beta_\mu)}{n_2\cos(\pi-\beta+\beta_\mu)} \tag{29}$$

$$F_{CF} = F_{BF} - \frac{F_o\cos(\pi+\alpha-\phi-\phi_\mu)}{n_2\cos(\pi-\phi-\phi_\mu)} \tag{30}$$

From equations (28) to (30), δ_{AB} and δ_{BC}, the axial shortened length of links 1 and 2, may be expressed by

$$\delta_{AB} = \frac{F_{AB}L_1}{A_1E_1} \tag{31}$$

$$\delta_{BC} = \frac{F_{CF}L_4\cos\gamma}{A_2E_2} + \frac{F_{BF}(L_2-L_4\cos\gamma)}{A_2E_2} \tag{32}$$

where A_i and E_i $(i=1,2)$ are the cross-sectional area and Young's modulus of links 1 and 2 respectively.

The elongation of the tie bars, U_c, given in equation (16), may be expressed by

$$U_c = \frac{F_cL_c}{n_cA_cE_c} \tag{33}$$

where F_c is the total tension of the tie bars given in equation (25), L_c is the length of the tie bars, n_c is the number of tie bars and A_c and E_c are the cross-sectional area and Young's modulus of the tie bars respectively. Substituting equations (31) to (33) into equation (16) gives

$$\frac{F_cL_c}{n_cA_cE_c} + \frac{F_{AB}L_1}{A_1E_1}\cos(\pi-\beta) + \left[\frac{F_{CF}L_4\cos\gamma}{A_2E_2} + \frac{F_{BF}(L_2-L_4\cos\gamma)}{A_2E_2}\right]\cos\alpha = \overline{U}_c \tag{34}$$

Using equations (22) to (24) gives

$$aF_{32}^2 - 2bF_{12}F_{32} + cF_{12}^2 = 0 \tag{35}$$

where

$$a = k_1^2 - k_3, \qquad b = k_1k_2 - k_3k_4, \qquad c = k_2^2 - k_3$$
$$k_1 = L_4\sin(\pi+\alpha+\gamma-\phi-\phi_\mu) + \rho_D$$
$$k_2 = L_2\sin(\pi+\alpha-\beta+\beta_\mu) + \rho_B$$
$$k_3 = \rho_C^2, \qquad k_4 = \cos(\phi+\phi_\mu-\beta+\beta_\mu) \tag{36}$$

From equation (35) and the inequality $M_{52} \geqslant 0$ given in equation (24),

$$\frac{F_{12}}{F_{32}} = \frac{a}{b+\sqrt{b^2-ac}} \tag{37}$$

From equations (18) to (21) and (37), the mechanical advantage M_a of the five-point double toggle mechanism may be obtained as

$$M_a = \frac{F_{cl}}{F_o} = \frac{a}{b+\sqrt{b^2-ac}}\frac{\cos(\pi-\beta+\beta_\mu)}{\cos(\pi-\phi-\phi_\mu)} \tag{38}$$

From equations (18) to (22) and (25),

$$F_c + F_o = F_{cl} \tag{39}$$

After substituting equations (28) to (30) into equation (34), the relationship of the total deformational force of the tie bars F_c, the clamping force F_{cl} and the necessary thrust applied to the crosshead F_o can be obtained from equations (34), (38) and (39).

For a specified final clamping force, the final total deformational force of the tie bars and the thrust applied to the crosshead can be obtained from equations (38) and (39). Then, the final deformations for links 1 and 2 and the tie bars can be calculated from equations (28) to (33). Then, using equations (11), (12), (16) and (17), the values of α_c, β_c and ϕ_c required at the beginning of the real mould clamping operation can be determined.

4 PARAMETRIC STUDIES

A conventional five-point double-toggle mechanism used in an injection-moulding machine serves as the object of improvement in the parametric study. The geometric properties are as follows: $L_1 = 231$ mm, $A_1 = 2184$ mm^2 and $n_1 = 6$ for links 1; $L_2 = 164$ mm, $L_4 = 133.17$ mm, $\gamma_C = 28.49°$, $A_2 = 3276$ mm^2, $n_2 = 4$, $r_B = 22.5$ mm, $r_C = 22.5$ mm, $r_D = 15.0$ mm, $R_B = 42$ mm and $R_D = 29$ mm for links 2; $L_3 = 70.04$ mm and $n_3 = 2$ for links 3; $n_4 = 1$ for the crosshead; $L_c = 1250$ mm, $A_c = 2827$ mm^2 and $n_c = 4$ for the tie bars; $d_A = 5$ mm, $d_E = 135$ mm, $d_0 = 235$ mm, $d_f = 350$ mm, $h_{CE}^{0^*} = 101.44$ mm, $e_1 = 47$ mm and $e_2 = 81$ mm, where R_B and R_D are the semi-widths of links 1 and the crosshead links respectively (see Figs 1 and 2);

d_0 is the vertical distance between the centre-line of the machine and point C; d_f is the vertical distance between the centre-line of the machine and the upper surface of the frame; e_1 and e_2 will be introduced in section 6. The superscript * is used only for the original mechanism. Young's modulus of the toggle links made of ductile irons is 172 GPa (17 593 kgf/mm^2) and Young's modulus of the tie bars made of Cr–Mo steels is 204 GPa (20 800 kgf/mm^2). The input stroke $\tilde{S}_E^*$ is 215.23 mm and the output stroke $\tilde{S}_A^*$ is 180.67 mm for this mechanism. When the final total deformational force of the tie bars $\tilde{F}_c = 539$ kN (55 000 kgf) is considered, it is possible to obtain, using the elastostatic model, the variations of the necessary thrust applied to the crosshead with angle α, shown in Fig. 7 for several friction coefficients under consideration and neglecting the deformational effect of the toggle linkage. It can be seen from Fig. 7 that a maximum thrust $F_{o,\max}$ is necessary to drive the crosshead and the effects of the hinge friction and the deformational effect of the toggle linkage should not be neglected for the real mould clamping operation. If both factors are neglected, the maximum thrusts are underestimated by about 45.5 and 60.5 per cent for the friction coefficients 0.05 and 0.1 respectively.

Without changing the specifications of the mould clamping force and the ejector unit, the space between the tie bar and the maximum allowable mould thickness and the stationary mould platen for the object of improvement, let A_1, A_2, A_c, n_1, n_2, n_3, n_c, r_B, r_C, r_D, R_B, R_D, e_1, e_2, d_A, d_E, d_0, d_f, T_m, T_s (see Figs 1 and 2) and $L_1 + L_2$ be invariable in the parametric study. For comparison, the final orientation of the crosshead link, $\tilde{\phi} = 92°$, will be kept invariable. Moreover, the friction coefficient in the pin joints during the real mould clamping process is assumed to be 0.1 and the final total deformational force of the tie bars $\tilde{F}_c = 539$ kN (55 000 kgf) is considered. Let $\tilde{S}_A = \tilde{S}_A^*$ and $\tilde{S}_E = \tilde{S}_E^*$ for case (a), $\tilde{S}_A = \tilde{S}_A^*$ and $\tilde{S}_E = 0.7\tilde{S}_E^*$ for case (b) (time saving) and $\tilde{S}_A = 1.4\tilde{S}_A^*$ and $\tilde{S}_E = \tilde{S}_E^*$ for case (c) (larger opening stroke). Also let L_1/L_2 be 1.6–0.6 with a decrement 0.1 and then let the value of L_4/L_2 vary from 1.2 to 0.3 with a decrement 0.01 to find the profiles of the toggle linkages of two types with a minimum value of $F_{o,\max}$, denoted by $F_{o,\max}^p$, in each case of L_1/L_2. Therefore, the profiles of the toggle linkages can be obtained for the two types with characteristics of time saving or larger opening stroke and/or thrust saving.

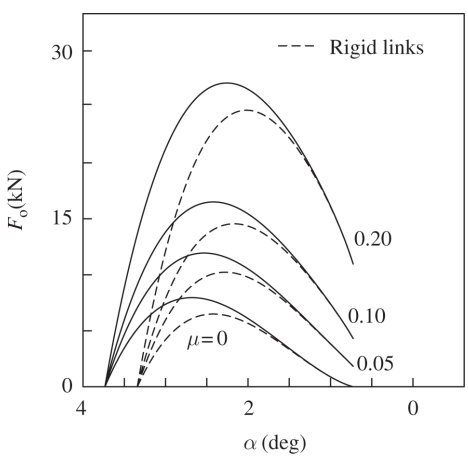

Fig. 7 Thrust applied to the crosshead versus angle α showing the two effects

5 INTERFERENCES

For the conventional five-point double-toggle type, in order to prevent the interference between the toggle linkages of two sets, the profiles of the two sets obtained by the parametric study may satisfy the following conditions with the minimum clearance 6 mm between the two sets. If $\alpha_0 + \gamma_C < \pi/2$, then check

$$L_2 \sin\alpha_0 + R_B < d_0 - 3 \quad \text{and}$$
$$L_4 \sin(\alpha_0 + \gamma_C) + R_D < d_0 - 3 \tag{40}$$

If $\alpha_0 < \pi/2$ and $\alpha_0 + \gamma_C \geqslant \pi/2$, then check

$$L_2 \sin\alpha_0 + R_B < d_0 - 3 \quad \text{and} \quad L_4 + R_D < d_0 - 3 \tag{41}$$

If $\alpha_0 \geqslant \pi/2$, then check

$$L_2 + R_B < d_0 - 3 \quad \text{and} \quad L_4 + R_D < d_0 - 3 \tag{42}$$

For the Fanuc five-point double-toggle type, in order to prevent the interference between the toggle linkages of two sets, the profiles of the toggle linkages obtained by the parametric study may satisfy the following conditions. If $\alpha_0 < \pi/2$, then check

$$L_2 \sin\alpha_0 + R_B < d_0 - 3 \quad \text{and}$$
$$L_4 \sin(\alpha_0 - \gamma_C) + R_D < d_0 - 3 \tag{43}$$

If $\alpha_0 \geqslant \pi/2$ and $\alpha_0 - \gamma_C < \pi/2$, then check

$$L_2 + R_B \leqslant d_0 - 3 \quad \text{and}$$
$$L_4 \sin(\alpha_0 - \gamma_C) + R_D < d_0 - 3 \tag{44}$$

If $\alpha_0 - \gamma_C \geqslant \pi/2$, then check

$$L_2 + R_B \leqslant d_0 - 3 \quad \text{and} \quad L_4 + R_D \leqslant d_0 - 3 \tag{45}$$

If the crosshead links shown in Fig. 2 interfere with links 1 situated in the middle position (see Fig. 3), when the crosshead retreats to the position for the maximum mould opening stroke, the links 1 situated in the middle position will be removed, so that the number of links 1 is equal to four. Then, the cross-sectional area

(i.e. the thickness) of each link 1 will be increased 1.5 times for comparison. Besides, the additional condition given below for the Fanuc five-point type may be satisfied to prevent the interference between the crosshead link and the frame of the machine:

$$L_3 \cos\left(\tilde{\phi} - \frac{\pi}{2}\right) + R_D < d_f + d_E - d_0 - 5 \tag{46}$$

where the minimum clearance between them is taken to be 5 mm. To raise the mechanical advantage of the Fanuc five-point type, the ratio of L_4 to L_2 may be increased, as a result of which it is probable that the interference between the crosshead link and the frame will occur. In this study, by increasing the height of the support block underlying the platen rather than the size of the platen, the interference will be prevented and the quality of the moulding will not be influenced. If the size of the platen is increased, reduction of the mould clamping mechanism in size and weight is hindered. Moreover, during the real mould clamping operation only the upper and lower end portions of the moving platen are pressed strongly. In the case where a mould to be attached is small sized, the moving platen may be curved; furthermore, this curvature may prevent a satisfactory mould clamping force from being transmitted to the central portion of the mould, thus possibly causing defective moulding [**3**]. In this study, to bring the performance of the Fanuc five-point type into full play, the condition of equation (46) will be loosened for some cases, but the necessary increment of the overall height of the machine ΔT_v will be shown. Thus, the increment of the height of the support block underlying the platen is $\frac{1}{2}\Delta T_v$.

6 OVERALL LENGTH OF THE MECHANISM

The pin joint A is pivotally mounted on the flange (projection) of the moving platen. An ejector unit is fixed to the moving platen. Let h_{ej} denote the nearest horizontal distance (see Fig. 8) between point B and the left end of the ejector unit having a horizontal distance e_1 with the point A during the mould closing (or opening) process. From Fig. 8, it can be seen that

$$h_{ej} = L_1 \sin\overline{\beta} - e_1 \tag{47}$$

$$\overline{\beta} = \begin{cases} \beta_0 - \dfrac{\pi}{2} & \text{if } \alpha_0 < \dfrac{\pi}{2} \\ \cos^{-1}\left(\dfrac{L_2 - d_A}{L_1}\right) & \text{if } \alpha_0 \geqslant \dfrac{\pi}{2} \end{cases} \tag{48}$$

where e_1 is measured positive, as shown in Fig. 8. Let h denote the horizontal nearest distance between point B and the left end of the ejector unit with the perpendicular clearance 5 mm between the right side of the links 1 and the left bottom end of the ejector unit, as shown in Fig. 8. Then

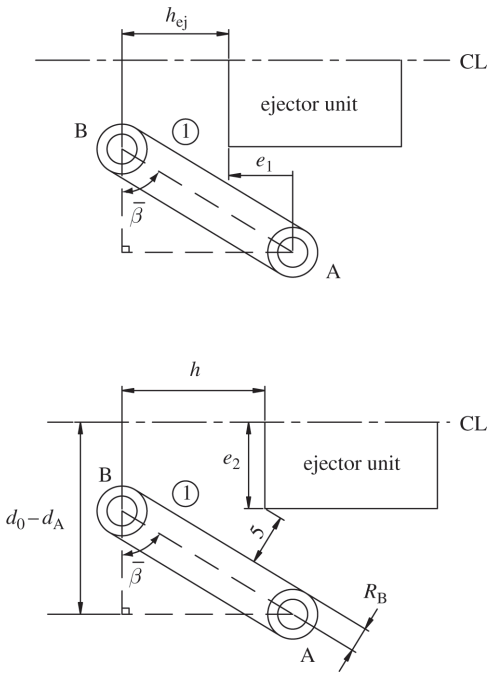

Fig. 8 Geometries with the horizontal nearest distances between point B and the ejector unit for the two conditions

$$h = L_1 \sin\overline{\beta} + (R_B + 5)\sec\overline{\beta} - (d_0 - d_A - e_2)\tan\overline{\beta} \tag{49}$$

where e_2 is the vertical distance between the centre-line of the machine and the bottom end of the ejector unit and $\overline{\beta}$ is given in equation (48).

The value of h is adopted as a standard to avoid interference between the links and the ejector unit. In some cases of this study (e.g. $L_1 < L_2$), if the space is not enough for the ejector unit, the horizontal length of the flange of the moving platen will be lengthened. The following should be checked:

$$\Delta h = h_{ej} - h \tag{50}$$

If the value of Δh is positive, this indicates that the space is enough for the ejector unit, so the horizontal length of the flange of the moving platen can be decreased by Δh, but without exceeding an allowable value, say 30 mm for the object of improvement. If the value of Δh is negative, the method of increasing the horizontal length of the flange of the moving platen by $-\Delta h$ is adopted.

The pin joint C is pivotally mounted on the flange of the tailstock platen. Thus, the horizontal length of the flange of the tailstock platen is the summation of h^0_{CE} given in equation (10) and a given value of clearance. Let Δh^0_{CE} denote the difference between h^0_{CE} and h^{0*}_{CE}, i.e.

$$\Delta h^0_{CE} = h^0_{CE} - h^{0*}_{CE} \tag{51}$$

If the value of Δh^0_{CE} is negative in some cases of this study (e.g. $L_1 < L_2$), this indicates that the horizontal length of the flange of the tailstock platen can be decreased by Δh^0_{CE}, but without exceeding an allowable value, say 180 mm for the object of improvement. Because the values of d_A, d_0 and $L_1 + L_2$ remain invariable, the distance between point A and point C in the final position is also invariable. Therefore, variations of the overall horizontal lengths of the mechanisms ΔT_h obtained in the study can be expressed as

$$\Delta T_h = \Delta h^0_{CE} - \Delta h \tag{52}$$

7 TRANSMISSION AND BUFFER CHARACTERISTICS

Most of the injection-moulding machines have three-step to five-step adjustment of the mould closing speed. To prevent mould damage, the velocity of the crosshead at the stage of contact between the moving mould and the stationary mould is always reduced to a very low value. Upon contacting, the velocity and acceleration of the moving platen suddenly drop to zero, thereby resulting in the impact and shock. The condition of a high contact velocity and acceleration represents an unsound buffer characteristic of the mechanism. They should be checked. In this study, the velocity of the crosshead for the mould closing operation is given below. The times for the first stage with a constant acceleration of 120 mm/s^2, the second stage with a constant velocity of 60 mm/s and the third stage with a constant deceleration of 120 mm/s^2 are 0.5, 1.5 and 0.25 s respectively. The time for the fourth stage with a constant velocity of 30 mm/s until the occurrence of the contact is determined by the initial position and the contact position. The symbols of a^0_A, v^c_A, and a^c_A denote the initial acceleration, the contact velocity and the contact acceleration of the moving platen respectively.

The condition of a high and maximum initial acceleration of the moving platen during the mould closing operation will appear in some cases, e.g. $L_1 < L_2$, where the mechanical advantage of the toggle linkage at the initial position is a very small minimum value smaller than 1.0. Thus, such a condition might result in the necessary thrust F^0_o at the beginning of the mould clamping operation exceeding the maximum thrust $F_{o,\,max}$ during the real mould clamping operation, and may be considered as an unsound transmission characteristic of the mechanism; such a condition should be avoided. In some cases where a small and maximum acceleration might appear at the early stage of the mould closing process very near the initial position, the mechanical advantage may not be a minimum value and then the difference of the thrust between the position with the maximum acceleration and the initial position may be slight compared to the value of $F_{o,\,max}$. Thus, the toggle linkage obtained by the parametric study should satisfy the following condition:

$$F^0_o = \frac{m_6(a^0_A + g\mu_s)}{M^0_a} < F_{o,\,max} \tag{53}$$

where m_6 is the mass of the moving platen with the ejector unit and the moving mould, M^0_a is the mechanical advantage of the toggle linkage at the initial position, g is the acceleration of gravity and μ_s is the static friction coefficient at the slider connection for the moving platen. In this study, the values of m_6 and μ_s are 220 kg and 0.125 respectively. The static friction coefficient in pin joints is 0.125 for M^0_a.

8 RESULTS AND DISCUSSION

The variations of $F^p_{o,\,max}/F^*_{o,\,max}, a^0_A, v^c_A, a^c_A, \Delta T_h$ and ΔT_v with L_1/L_2 for case (a) are shown in Table 1. It can be seen from Table 1 that the value of $F^p_{o,\,max}$ for the Fanuc five-point type is up to about 31 per cent smaller than the one for the conventional five-point type. The differences of $F^p_{o,\,max}$ between the two types can reach about 35, 37 and 39 per cent if the overall height of the Fanuc five-point type increases by 51.0, 120.0 and 178.4 mm respectively. It seems that the effect of reducing the thrust is not remarkable when the overall height of the Fanuc type is increased. Moreover, the values of $F^p_{o,\,max}$ become lower with a decrease in L_1/L_2 for either the conventional or the Fanuc five-point type. The reductions of the thrust $F^p_{o,\,max}$ for the conventional and Fanuc five-point types reach only about 4 and 10 per cent respectively; on the other hand, the overall horizontal lengths of the mechanisms of the two types can be decreased by about 30 mm.

The variations of $F^p_{o,\,max}/F^*_{o,\,max}, a^0_A, F^0_o/F^p_{o,\,max}, v^c_A, a^c_A$ and ΔT_h with L_1/L_2 for case (b) are shown in Table 2. It can be seen from Table 2 that the value of $F^p_{o,\,max}$ for the Fanuc five-point type is about 5–19 per cent smaller than the one for the conventional five-point type. Once again, the values of $F^p_{o,\,max}$ become lower with a reduction in L_1/L_2 for either the conventional or the Fanuc five-point type. Note that the effect of thrust saving for the Fanuc type does not become manifested in the case of $L_1/L_2 > 1.1$ for time saving. The differences of $F^p_{o,\,max}$ between the two cases of $L_1/L_2 =$ 1.6 and 0.7 for the conventional and the Fanuc five-point types can reach about 22 and 30 per cent respectively. However, in the case of $L_1/L_2 = 0.6$ in Table 2, the initial acceleration of the moving platen and the initial thrust F^0_o applied to the crosshead become very large, so toggle linkages of this kind should not be adopted. On the other hand, the increments of the overall horizontal lengths between the two cases of

Table 1 Geometric and kinematic parameters corresponding to $F^p_{o,\,max}$ in each L_1/L_2 for case (a)

Conventional five-point type with $\widetilde{S}_E = \widetilde{S}^*_E$ and $\widetilde{S}_A = \widetilde{S}^*_A$

L_1/L_2	L_4/L_2	γ_C (deg)	L_3 (mm)	$F^p_{o,\,max}/F^*_{o,\,max}$ (%)	a^0_A (mm/s^2)	v^c_A (mm/s)	a^c_A	ΔT_h (mm)	$F^0_o/F^p_{o,\,max}$ (%)
1.6	0.77	28.24	78.40	98.41	208.9	1.3	−3.4	−15.8	3.5
1.5	0.78	27.62	76.53	97.99	195.7	1.3	−3.4	−22.0	3.3
1.4	0.80	26.35	75.12	96.64	186.3	1.3	−3.3	−30.8	3.2
1.3	0.85	24.96	71.77	94.66	177.5	1.3	−3.2	−45.3	3.1

Fanuc five-point type with $\widetilde{S}_E = \widetilde{S}^*_E$ and $\widetilde{S}_A = \widetilde{S}^*_A$

L_1/L_2	L_4/L_2	γ_C (deg)	L_3 (mm)	$F^p_{o,\,max}/F^*_{o,\,max}$ (%)	a^0_A (mm/s^2)	v^c_A (mm/s)	a^c_A	ΔT_h (mm)	ΔT_v
1.6	0.87	37.50	214.26	73.68	177.3	1.1	−2.4	−14.6	0
1.5	0.88	36.18	215.78	71.35	189.8	1.1	−2.3	−21.9	0
1.4	0.88	33.80	214.16	69.37	204.4	1.0	−2.2	−30.1	0
1.3	0.89	32.05	214.59	67.24	221.7	1.0	−2.1	−39.3	0
1.2	0.90	29.92	213.95	65.36	242.6	1.0	−2.0	−43.6	0
1.1	0.92	28.38	215.46	63.41	269.7	1.0	−1.9	−42.9	0
1.0	1.00	33.36	241.65	60.81	313.6	0.9	−1.7	−44.1	51.0
1.0	1.10	41.19	276.15	58.70	322.2	0.9	−1.7	−41.9	120.0
1.0	1.20	46.63	305.40	57.14	328.5	0.9	−1.6	−40.5	178.4

$L_1 + L_2 = 395$ mm, $F^*_{o,\,max} = 16$ kN, $a^0_E = 120$ mm/s^2, $v^c_E = 30$ mm/s, $\mu = 0.1$.

Table 2 Geometric and kinematic parameters corresponding to $F^p_{o,\,max}$ in each L_1/L_2 for case (b)

Conventional five-point type with $\widetilde{S}_E = 0.7\widetilde{S}^*_E$ and $\widetilde{S}_A = \widetilde{S}^*_A$ (time saving)

L_1/L_2	L_4/L_2	γ_C (deg)	L_3 (mm)	$F^p_{o,\,max}/F^*_{o,\,max}$ (%)	a^0_A (mm/s^2)	$F^0_o/F^p_{o,\,max}$ (%)	v^c_A (mm/s)	a^c_A	ΔT_h (mm)
1.6	0.49	35.65	90.90	121.66	826.7	14.9	1.6	−4.9	−37.5
1.5	0.47	34.33	92.41	122.48	569.6	9.4	1.6	−5.0	−38.4
1.4	0.45	31.99	95.03	122.49	462.9	7.3	1.6	−5.1	−39.8
1.3	0.43	28.03	99.53	121.30	410.6	6.5	1.6	−5.1	−42.0
1.2	0.41	20.91	107.92	118.38	387.1	6.3	1.6	−5.0	−39.2
1.1	0.40	10.47	120.46	113.72	388.2	6.6	1.6	−4.8	−31.3
1.0	0.42	13.79	114.28	113.56	412.4	7.2	1.6	−4.7	−24.5
0.9	0.44	11.86	115.13	110.77	452.3	8.4	1.5	−4.5	−19.0
0.8	0.47	8.89	117.83	106.58	530.9	11.0	1.5	−4.2	−15.4
0.7	0.51	1.76	129.95	99.36	724.5	18.8	1.4	−3.8	−13.1
0.6	0.59	1.89	128.44	93.81	1466.0	68.8	1.3	−3.4	−17.3

Fanuc five-point type with $\widetilde{S}_E = 0.7\widetilde{S}^*_E$ and $\widetilde{S}_A = \widetilde{S}^*_A$ (time saving)

L_1/L_2	L_4/L_2	γ_C (deg)	L_3	$F^p_{o,\,max}/F^*_{o,\,max}$ (%)	a^0_A (mm/s^2)	$F^0_o/F^p_{o,\,max}$ (%)	v^c_A (mm/s)	a^c_A	ΔT_h (mm)
1.6	0.63	57.99	215.65	116.57	240.2	3.6	1.7	−5.6	−25.0
1.5	0.62	55.91	215.55	111.95	258.8	4.1	1.6	−5.2	−29.2
1.4	0.61	53.72	215.30	107.77	280.0	4.7	1.5	−4.9	−33.7
1.3	0.60	51.39	214.83	103.96	304.5	5.4	1.5	−4.6	−38.6
1.2	0.59	48.85	214.01	100.67	333.5	6.3	1.5	−4.4	−37.8
1.1	0.59	46.91	215.21	97.59	369.0	7.4	1.4	−4.1	−31.0
1.0	0.59	44.71	216.05	94.69	415.7	8.9	1.4	−3.9	−24.5
0.9	0.58	41.02	213.11	92.34	481.2	11.1	1.4	−3.7	−18.3
0.8	0.59	38.71	214.80	89.45	587.4	15.1	1.3	−3.4	−12.4
0.7	0.60	35.22	214.08	86.73	803.7	25.1	1.3	−3.2	−6.7
0.6	0.62	30.54	211.22	83.82	1628.0	90.9	2.4	−3.0	−1.7

$L_1 + L_2 = 395$ mm, $F^*_{o,\,max} = 16$ kN, $a^0_E = 120$ mm/s^2, $v^c_E = 30$ mm/s, $\mu = 0.1$.

$L_1/L_2 = 1.6$ and 0.7 for the two types do not exceed about 25 mm.

The variations of $F^p_{o,\,max}/F^*_{o,\,max}$, a^0_A, $F^0_o/F^p_{o,\,max}$, v^c_A, a^c_A and ΔT_h with L_1/L_2 for case (c) are shown in Table 3. It can be seen from Table 3 that the value of $F^p_{o,\,max}$ for the Fanuc five-point type is up to about 25 per cent smaller than the one for the conventional five-point type. Again and again, the values of $F^p_{o,\,max}$ become lower with a decrease in L_1/L_2 for either the conventional or the Fanuc five-point type. The reductions of the thrust $F^p_{o,\,max}$ for the conventional and the Fanuc five-point types reach about 8 and 33 per cent respectively; on the

Table 3 Geometric and kinematic parameters corresponding to $F^{p}_{o,\,max}$ in each L_1/L_2 for case (c)

Conventional five-point type with $\tilde{S}_E = \tilde{S}^{*}_E$ and $\tilde{S}_A = 1.4\tilde{S}^{*}_A$ (larger opening stroke)

L_1/L_2	L_4/L_2	γ_C (deg)	L_3	$F^{p}_{o,\,max}/F^{*}_{o,\,max}$ (%)	a^{0}_{A} (mm/s^2)	$F^{0}_{o}/F^{p}_{o,\,max}$ (%)	v^{c}_{A} (mm/s)	a^{c}_{A}	ΔT_h (mm)
1.6	0.51	7.80	123.59	101.46	303.2	5.0	1.4	−3.8	11.5
1.5	0.50	3.21	129.66	100.31	231.4	3.8	1.4	−3.8	9.5
1.4	0.51	2.79	129.67	98.58	223.2	3.8	1.4	−3.7	4.5
1.3	0.53	5.48	125.24	97.22	230.4	4.0	1.4	−3.6	4.9
1.2	0.56	9.19	117.77	96.58	244.4	4.4	1.4	−3.5	15.1
1.1	0.60	10.05	113.97	94.36	265.0	5.0	1.4	−3.4	22.0
1.0	0.68	14.40	100.01	93.44	302.7	6.1	1.3	−3.3	22.2

Fanuc five-point type with $\tilde{S}_E = \tilde{S}^{*}_E$ and $\tilde{S}_A = 1.4\tilde{S}^{*}_A$ (larger opening stroke)

L_1/L_2	L_4/L_2	γ_C (deg)	L_3	$F^{p}_{o,\,max}/F^{*}_{o,\,max}$ (%)	a^{0}_{A} (mm/s^2)	$F^{0}_{o}/F^{p}_{o,\,max}$ (%)	v^{c}_{A} (mm/s)	a^{c}_{A}	ΔT_h (mm)
1.6	0.49	23.49	163.91	102.23	159.9	2.5	1.5	−4.1	20.9
1.5	0.68	49.61	216.07	97.35	137.1	2.2	1.4	−4.0	20.7
1.4	0.69	46.16	216.04	91.16	157.7	2.8	1.3	−3.6	11.6
1.3	0.70	42.48	215.19	85.98	183.0	3.6	1.3	−3.2	8.9
1.2	0.72	39.31	215.75	81.44	215.8	4.6	1.2	−2.9	16.6
1.1	0.74	35.47	214.46	77.32	263.5	6.2	1.2	−2.7	22.0
1.0	0.77	31.48	212.90	73.27	343.2	9.1	1.1	−2.4	25.1
0.9	0.82	27.76	212.61	68.92	521.2	17.3	1.0	−2.1	25.0

$L_1 + L_2 = 395$ mm, $F^{*}_{o,\,max} = 16$ kN, $a^{0}_{E} = 120$ mm/s^2, $v^{c}_{E} = 30$ mm/s, $\mu = 0.1$.

other hand, the increments of the overall horizontal lengths of the mechanisms of the two types do not exceed about 12 mm. Since the values of $L_1 + L_2$, d_A and d_E remain invariable, the final position of the mould clamping process is the same for all cases. In addition, since the final deformational forces $\tilde{F}_c$ are the same, the values of $\tilde{U}_c$ may also be the same. The smaller the value of L_1/L_2, the greater is the angle of swing from β_c to $\tilde{\beta}$ and the smaller is α_c. The smaller the value of α_c, the smaller are U_c and F_c for a given α. The above result can be seen in Fig. 9, which shows the curves of F_c versus angle α for the Fanuc five-point type. That is the major reason why the values of $F^{p}_{o,\,max}$ become lower with a decrease in L_1/L_2 for either the conventional or the Fanuc five-point type. Figure 10 shows the curves of the mechanical advantage M_a versus angle α for several values of L_1/L_2. Figure 11 shows the variations of the thrust F_o with the angle α for several values of L_1/L_2. It can be seen from Fig. 11 that the smaller the value of α_c, the smaller is the value of angle α corresponding to the maximum thrust.

The variations of $F_{o,\,max}/F^{*}_{o,\,max}$ with L_4/L_2 for the case of $L_1/L_2 = 1.1$ of case (c) are shown in Table 4. It can be seen from Table 4 that the values of $F_{o,\,max}$ for the conventional five-point type become lower with a reduction in L_4/L_2 of about 22 per cent. In contrast to the conventional five-point type, the values of $F_{o,\,max}$ for the Fanuc type increase with a reduction in L_4/L_2 of about 9 per cent. For a given L_1/L_2, the mechanical advantage may be considered as the combination of two

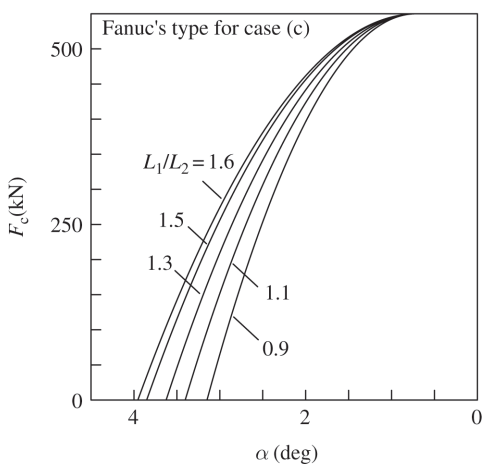

Fig. 9 Total deformational force of the tie bars versus angle α

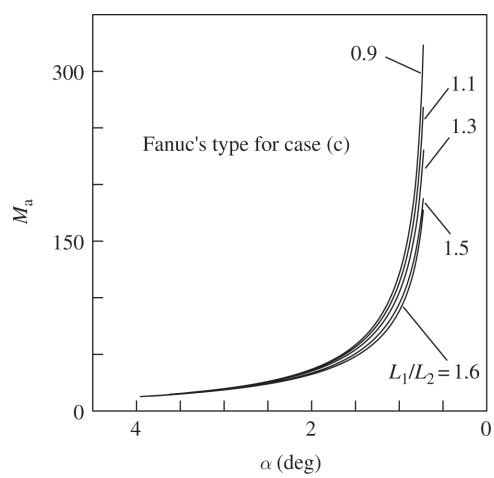

Fig. 10 Mechanical advantage versus angle α

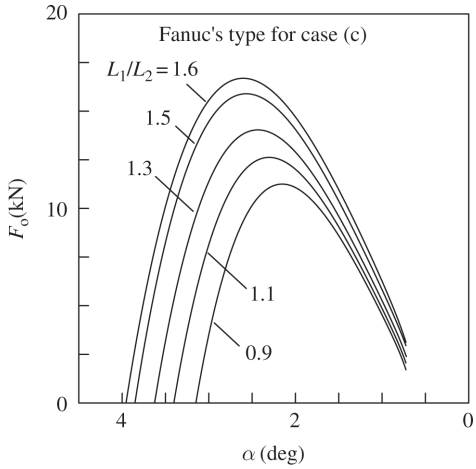

Fig. 11 Thrust applied to the crosshead versus angle α

major factors. One is k_1/k_2, the other is $1/\cos(\pi - \phi)$. The latter is dominant for both types of mechanisms. From all of the numerical results for a given L_1/L_2, the values of γ_C decrease for the two types with a reduction in L_4/L_2, and then the values of L_3 increase for the conventional type and decrease for the Fanuc type. Since the final orientation of the crosshead link is the same, the greater the value of L_3, the smaller is the angle of swing from ϕ_c to $\tilde{\phi}$ and then the greater is the value of $1/\cos(\pi - \phi)$. Thus, the values of $F_{o,\,max}$ for the conventional five-point type is lower with a reduction in L_4/L_2. However, the values of $F_{o,\,max}$ for the Fanuc five-point type increase with a reduction in L_4/L_2. Only one exception occurs in the case of the conventional and Fanuc types with $L_1/L_2 = 1.6$ in case (c) individually. However, the differences among the values of $F_{o,\,max}$ in the cases are very small, only up to about 0.1 and 2 per cent respectively.

It can be seen from Tables 1 to 3 that the impact velocity and acceleration are relatively small. Thus, the five-point double-toggle mechanism inherently has the buffer characteristic.

9 CONCLUSIONS

The elastostatic model using Coulomb friction for the five-point double-toggle clamping mechanism is presented in order to find the maximum thrust applied to the crosshead during the real mould clamping operation. The effects of the hinge friction and the deformational effect of the toggle linkage should not be neglected for the real mould clamping operation. If both factors are neglected, the maximum thrusts are underestimated by about 45.5 and 60.5 per cent for friction coefficients of 0.05 and 0.1 respectively, based on the present model.

The present study adopts lengthening the flange (projection) of the moving platen rather than the length of links 1 to provide enough horizontal space for the ejector unit, if necessary. In such a case, the length of the flange of the tailstock platen can be decreased. The variations of the overall horizontal lengths of the toggle mechanisms, whether for time saving or for a larger opening stroke as obtained in the present study, are acceptable.

Table 4 Geometric parameters and $F_{o,\,max}$ versus L_4/L_2 in the case of $L_1/L_2 = 1.1$ for case (c)

Two types of mechanisms with $\tilde{S}_E = 1.0\tilde{S}^*_E$, $\tilde{S}_A = 1.4\tilde{S}^*_A$ and $L_1/L_2 = 1.1$							
Conventional five-point type				Fanuc five-point type			
L_4/L_2	γ_C (deg)	L_3	$F_{o,\,max}/F^*_{o,\,max}$ (%)	L_4/L_2	γ_C (deg)	L_3	$F_{o,\,max}/F^*_{o,\,max}$ (%)
0.70	33.37	61.23	116.63	0.74	35.47	214.46	77.32
0.69	32.02	64.84	114.31	0.73	34.41	211.28	77.67
0.68	30.58	68.59	112.09	0.72	33.28	208.01	78.03
0.67	29.01	72.53	109.94	0.71	32.09	204.64	78.41
0.66	27.32	76.69	107.84	0.70	30.83	201.16	78.82
0.65	25.45	81.12	105.78	0.69	29.48	197.56	79.25
0.64	23.37	85.90	103.74	0.68	28.03	193.80	79.72
0.63	21.01	91.17	101.66	0.67	26.47	189.86	80.22
0.62	18.25	97.14	99.51	0.66	24.77	185.70	80.76
0.61	14.84	104.27	97.18	0.65	22.91	181.27	81.37
0.60	10.05	113.97	94.36	0.64	20.83	176.49	82.04
				0.63	18.47	171.22	82.81
				0.62	15.71	165.25	83.74
				0.61	12.30	158.12	84.90
				0.60	7.51	148.42	86.62

$L_1 + L_2 = 395$ mm, $F^*_{o,\,max} = 16$ kN, $\mu = 0.1$.

The present design for the conventional five-point type resulting from the parameter study enables the input stroke to be reduced by 30 per cent or the opening stroke to be increased by 40 per cent of the object of improvement, while decreasing the thrust by about 1 and 7 per cent respectively. On the other hand, the present design for the conventional five-point type enables the thrust of the object of improvement to be reduced by about 5 per cent, without changing the input and opening strokes. Adoption of the Fanuc five-point type according to the parameter study enables the input stroke to be reduced by 30 per cent or the opening stroke to be increased by 40 per cent of the object of improvement, while decreasing the thrust by about 13 and 31 per cent respectively. On the other hand, the adoption of the Fanuc five-point type enables the thrust of the improved mechanism to be reduced by about 37 per cent, without changing the input stroke and output strokes.

The Fanuc five-point type is much superior to the conventional five-point type in the thrust saving and/or larger opening stroke. The present study brings the performances of the Fanuc five-point type into full play. Note that the difference in the thrust between the two types minimizes to be 12 per cent in the time saving case.

The ratio of L_1 to L_2, whether for the conventional or for the Fanuc five-point type, should be as small as possible for thrust saving on condition that the geometry can be satisfied and the transmission characteristic can be accepted. Furthermore, the ratio of L_4 to L_2 should be as small as possible for the conventional five-point type but as great as possible for the Fanuc five-point type on condition that the geometry can be satisfied and the interference can be prevented. The present study can be directly applied to the five-point double-toggle clamping mechanism of a die-cast machine.

REFERENCES

1 **Smith, A.** *How to Choose a Plastics Injection Moulding Machine*, 1995 (AMI Business Publishing, Bristol).
2 **Johannaber, F.** *Injection Molding Machines*, 1994 (Hanser, New York).
3 **Ito, S.** and **Nishimura, K.** Mold clamping mechanism of an injection molding machine. US Pat. Doc. 5843496, 1998.
4 **Norton, R. L.** *Design of Machinery*, 1999 (McGraw-Hill, New York).
5 **Burton, P.** *Kinematics and Dynamics of Planar Machinery*, 1979 (Prentice-Hall, Englewood Cliffs, New Jersey).
6 **Wilson, C. E., Sadler, J. P.** and **Michels, W. J.** *Kinematics and Dynamics of Machinery*, 1983 (Harper and Row, New York).